

Morphological Number Counts of Galaxies in the Hubble Deep Field South

By

Myung Gyoon LEE* and Narae HWANG*

(November 1, 2000)

Abstract: We present a study of photometric properties of the galaxies in the Hubble Deep Field South (HDFS) based on the released WFPC2 images obtained with the Hubble Space Telescope (HST). We have classified about 340 galaxies with $I < 26$ mag in the HDFS as well as about 400 galaxies in the Hubble Deep Field North (HDFN) using the visual classification supplemented by inspection of the surface brightness profiles of the galaxies. Galaxy population statistics and morphological number counts for the HDFS are found to be similar to those for the HDFN. We have also determined photometrically the redshifts of the galaxies with $I < 26$ mag in the HDFS and the HDFN using the empirical training set method. Redshift distribution, color-redshift relation, and magnitude-redshift for each type of galaxies are investigated.

1. INTRODUCTION

Hubble Deep Field Program has provided us with the deepest images presently possible which are very useful as windows to understand the formation and evolution of the distant universe (Ferguson, Dickinson & Williams 2000). Following the Hubble Deep Field North (HDFN), the Hubble Deep Field South was observed with WFPC2, NICMOS and STIS in October 1998 (Williams et al. in preparation). We have analyzed the WFPC2 data among them, and have classified bright galaxies with $I < 26$ mag. Here we present a preliminary study of various aspects of the galaxies in the HDFS including morphology, number counts, redshift, and colors in comparison with the HDFN.

2. PHOTOMETRY

We have used a galaxy photometry software FOCAS (Faint Object Classification and Analysis System) (Valdes et al. 1995) to detect the objects and to obtain the photometry of the detected objects in the WFPC2 images. We have combined B , V and I images released to the community to create a master image which is used for final object detection with FOCAS. Williams et al. (1996) also used FOCAS for the photometry of the galaxies in the HDFN, while

* Astronomy Program, SEES, Seoul National University, Shillim-Dong Kwanak-Gu, Seoul 151-742, South Korea; mglee@astrog.snu.ac.kr

Williams et al. (in preparation) used the Source Extractor (SExtractor) (Bertin & Arnouts 1996) for the photometry of the galaxies in the HDFs. Details of the photometry are described in Hwang (2000). Finally, we have obtained the photometry of about 2400 objects reaching $V \sim 30$ mag in the HDFs, and of about 2700 objects in the HDFN. A comparison of our photometry with the photometry given by Williams et al. (in preparation) shows that they agree well in general and that the FOCAS magnitudes get somewhat brighter than the SExtractor magnitudes at the faint level ($V > 28$ mag).

Figure 1 displays an I vs. $(V - I)$ color-magnitude diagram of the measured objects in the HDFs. Several features are seen in Figure 1: galaxies start to appear at $I \sim 21$ mag; most galaxies are bluer than $(V - I) \sim 1.0$; and galaxies get bluer progressively as they get fainter. These features are, in general, similar to those for the HDFN.

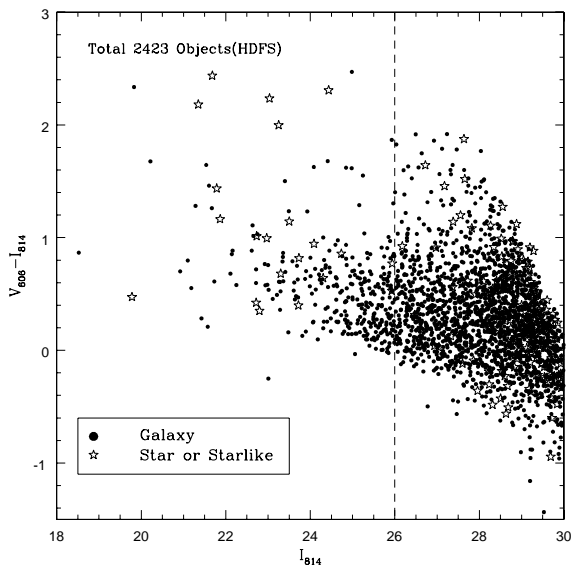


Fig. 1: I vs. $(V - I)$ color-magnitude diagram of the measured objects in the HDFs. The dashed line at $I = 26$ mag represents the magnitude limit for morphological classification.

3. MORPHOLOGICAL CLASSIFICATION AND NUMBER COUNTS

3.1 Method

Morphological characteristics of faint galaxies provide critical information for understanding the evolution of galaxies. However, it is very difficult to classify galaxies in the HDF, and the results published so far are diverse (see Ferguson et al. 2000). We have classified the bright galaxies with $I < 26$ mag in the HDFs as well as in the HDFN. For morphological classification we have used visual classification supplemented with inspection of the surface brightness profiles of the objects. We have fit the surface brightness profiles of the objects with de Vaucouleurs law, exponential law and King models. Figure 2 displays the surface brightness profiles of typical early-type and late-type galaxies.

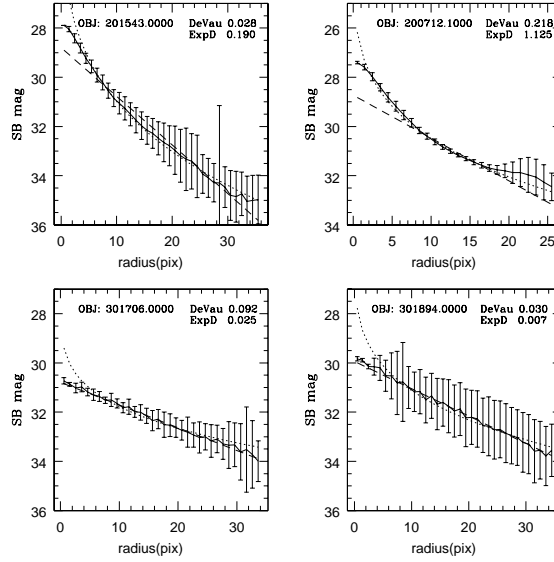


Fig. 2: Surface brightness profiles of a sample of early-type (upper panels) and late-type (lower panels) galaxies. The dotted line and the dashed line represent fits to the data with the de Vaucouleurs law and exponential law, respectively. One pixel in radius corresponds to 0.0398 arcsec.

3.2 Results

One of the well-known difficulties in classification of faint galaxies in the HST images is due to splitting of a single galaxy into several bodies or merging of a few galaxies into one body by the softwares used. No known softwares including FOCAS and SExtractor can take care of this problem perfectly. We have inspected each image visually to handle this problem. It is very time and labor-consuming, but provides reasonably reliable results.

Finally, we have classified about 340 galaxies in the HDFs and about 400 galaxies in the HDFN into four classes: early-type, late-type (spirals), peculiar/irregular, and merger. The classification schemes are basically similar to those used by van den Bergh et al. (1996), but we used surface photometry of galaxies as well for classification. A comparison of our results for the HDFs with those of van den Bergh et al. shows a good agreement between the two.

Figure 3 illustrates the morphological population statistics for the classified objects in the HDFs in comparison with those in the HDFN. It is found that galaxy population statistics are similar between the HDFs and the HDFN: the most dominant population in the HDFs is peculiar/irregular galaxies, and the late type galaxies are somewhat more than the early type galaxies. However, the number of stars in the HDFs is about twice that in the HDFN, which is consistent with the result given by Mendez & Minniti (2000). It is as expected, because the HDFs is closer to the center of our Galaxy than the HDFN.

We have then derived the I -band number counts of each type of galaxies with $I < 26$ mag, and they are displayed in Figure 4. Figure 4 shows that the number counts for the HDFs agree in general with those for the HDFN, and that the number counts of the peculiar/irregular galaxies are steeper than those of the early-type and late-type galaxies both of which are similar to each other. The number of the peculiar/irregular galaxies is larger than those for the other types at $I > 24.5$ mag. Both of the early-types and late-types in the both fields show a slight

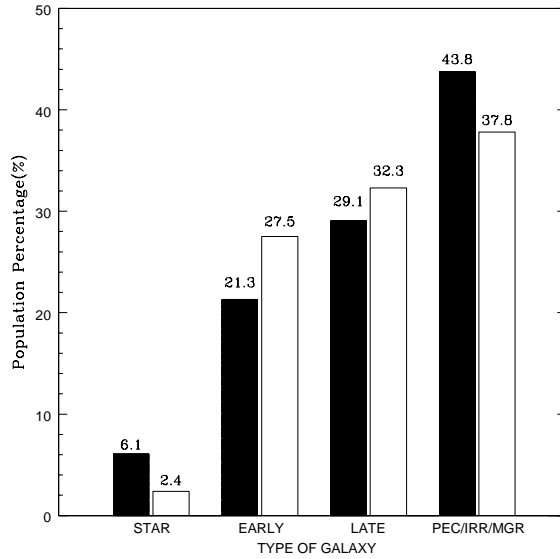


Fig. 3: Morphological population statistics of the objects with $I < 26$ mag in the HDFs (black bars) and the HDFN (white bars).

dip at $I \sim 23.8$ mag, which needs further investigation.

4. PHOTOMETRIC REDSHIFTS

We have determined photometrically the redshifts of about 340 galaxies with $I < 26$ mag in the HDFs and of about 400 galaxies in the HDFN using the empirical training set method described in Wang et al. (1998, 1999). Wang et al. presented the calibration for the empirical training set based on 82 galaxies with measured spectroscopic redshifts $0.1 < z < 3.5$ in the HDFN. Some galaxies detected in the master image are too faint to be detected in the U image. A value of $U = 30$ mag was assumed as an upper limit for such U -band limited galaxies in determining the photometric redshift so that the redshifts of these galaxies are more uncertain than those for the other galaxies.

Figure 5 displays the redshift distribution of all the galaxies with $I < 26$ mag in the HDFs in comparison with that for the HDFN, and Figure 6 illustrates the redshift distribution of each type of the galaxies with $I < 26$ mag. A comparison of our results with those given for the galaxies with $I < 26$ mag in the HDFN given by Driver et al. (1998) shows a reasonably good agreement between the two.

Several distinguishable features are seen in Figures 5 and 6: a) The HDFs data show three strong peaks, at $z \sim 0.5$, 1.0, 1.9, and one weaker peak at $z \sim 2.7$, while the HDFN data show one prominent peak at $z \sim 0.8$, one weak peak at $z \sim 1.8$, and a marginal peak at $z \sim 2.7$. The difference in the strongest peak between the HDFs and HDFN is due to the stronger concentration of early-type and late-type galaxies within $z \sim 1.2$ in the HDFN as compared to the HDFs, as shown in Figure 6; b) The numbers of early-type and late-type galaxies in the HDFN decrease suddenly at $z \sim 1.2$ and to a less degree at $z \sim 2.1$, while those for the HDFs decrease more gradually with increasing redshift. This, with the point in a), indicates that the

evolutionary history of the galaxies in the HDFN and the HDFS might have been different; and c) the merger and peculiar/irregular type galaxies show, on an average, larger redshifts than those of the late-type and early-type galaxies, which is seen more clearly in the HDFN than in the HDFS. This shows that mergers were more frequent before the main population of the late-type and early-types.

Figure 7 displays morphological color–redshift diagrams of the galaxies with $I < 26$ mag in the HDFS. The colors vary significantly with increasing redshift. For example, $(V - I)$ colors get redder for $0 < z < 1.0$, show a peak at $z \sim 1.0$, get bluer for $1.0 < z < 2$, and get redder again for $z > 2.5$. One interesting point seen in Figure 7 is that the color range of early-type galaxies at $z < 1$ in the HDFS (and the HDFN) is very large from $(B - V) \sim 0.0$ to ~ 1.8 , suggesting that the star formation histories in early-type galaxies have been very diverse.

Figure 8 displays morphological magnitude–redshift diagrams of the galaxies with $I < 26$ mag in the HDFS. Figure 8 shows, in general, a distance effect on the redshift, i.e., the brightest galaxies get fainter with increasing redshift. However, there appears to be a turn-over in this trend around $z \sim 3$ (even excluding the U -band limited galaxies). It will be interesting to confirm the redshifts of the brightest galaxies at $z \sim 3$.

5. SUMMARY

We have investigated several photometric properties of the galaxies with $I < 26$ mag in the HDF in comparison with the HDFN. We have applied the same procedures for both the HDFS and HDFN for direct comparison, so that the relative differences we find between the two fields must be reliable. Next step will be to interpret the results by modelling the formation and evolution of galaxies. Since the invaluable data for the HDFN and HDFS were released, many papers have been published using these data. However, there are still significant differences and/or conflicts as well as agreements among the results (even among the data, excluding any models), showing clearly how difficult it is to mine the truth in the field (see Ferguson et al. 2000 and references therein). This indicates that other kinds of data in addition to the HDF data are needed for achieving the final goal of understanding the formation and evolution of galaxies. In this sense HDFS and HDFN are also very interesting targets for the coming infrared missions including ASTRO-F and HII/L2.

ACKNOWLEDGMENT

This research is in part supported by the BK21 program of the Korean Government.

REFERENCES

- Bertin, E. & Arnouts, S. 1996, A&AS, 117, 393
- Driver, S.P. et al. 1998, ApJ, 496, L93
- Ferguson, H.C., Dickinson, M., & Williams, R. 2000, AR&AA, in press
- Hwang, N. 2000, M.S. Thesis, Seoul National University
- Mendez, R.A., & Minniti, D. 2000, ApJ, 529, 911
- Valdes, F.G. et al. 1995, PASP, 107, 1119
- van den Bergh, S. et al. 1996, AJ, 116, 2081
- Wang, Y., Bahcall, N., & Turner, E.L. 1998, AJ, 116, 2081
- Wang, Y., Bahcall, N., & Turner, E.L. 1999, preprint(astro-ph/9906256)
- Williams, R. et al. 1996, AJ, 112, 1335

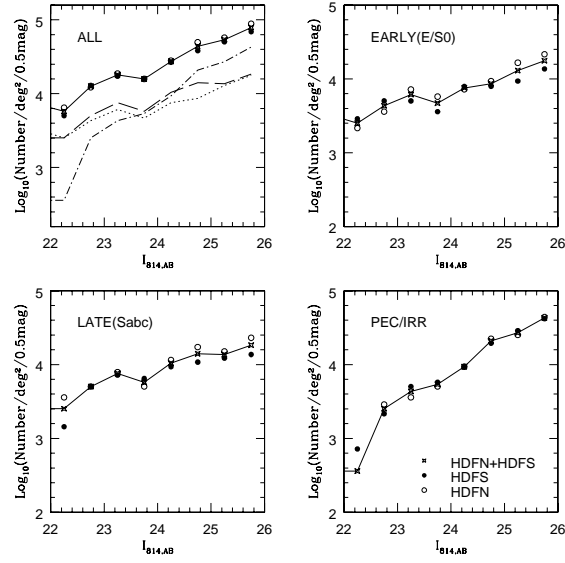


Fig. 4: Morphological number counts at I -band of the galaxies with $I < 26$ mag in the HDFS (the filled circles) and the HDFN (the open circles). The solid line represents the mean of the HDFS and the HDFN. The long-dashed line, short-dashed line and dot-dashed line in the left upper panel represent, respectively, the late-type, early-type and peculiar/irregular galaxies.

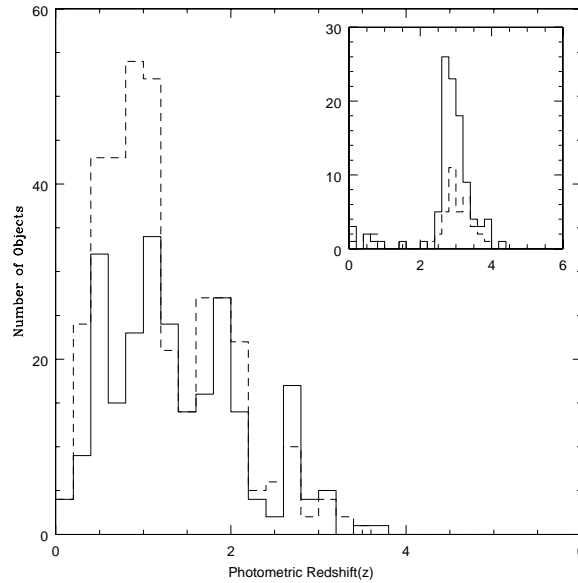


Fig. 5: Photometric redshift distribution of the galaxies with $I < 26$ mag in the HDFS (the solid line) and the HDFN (the dashed line). The inlaid box represents the redshift distribution of the U -band limited galaxies whose redshift estimates are more uncertain than for others.

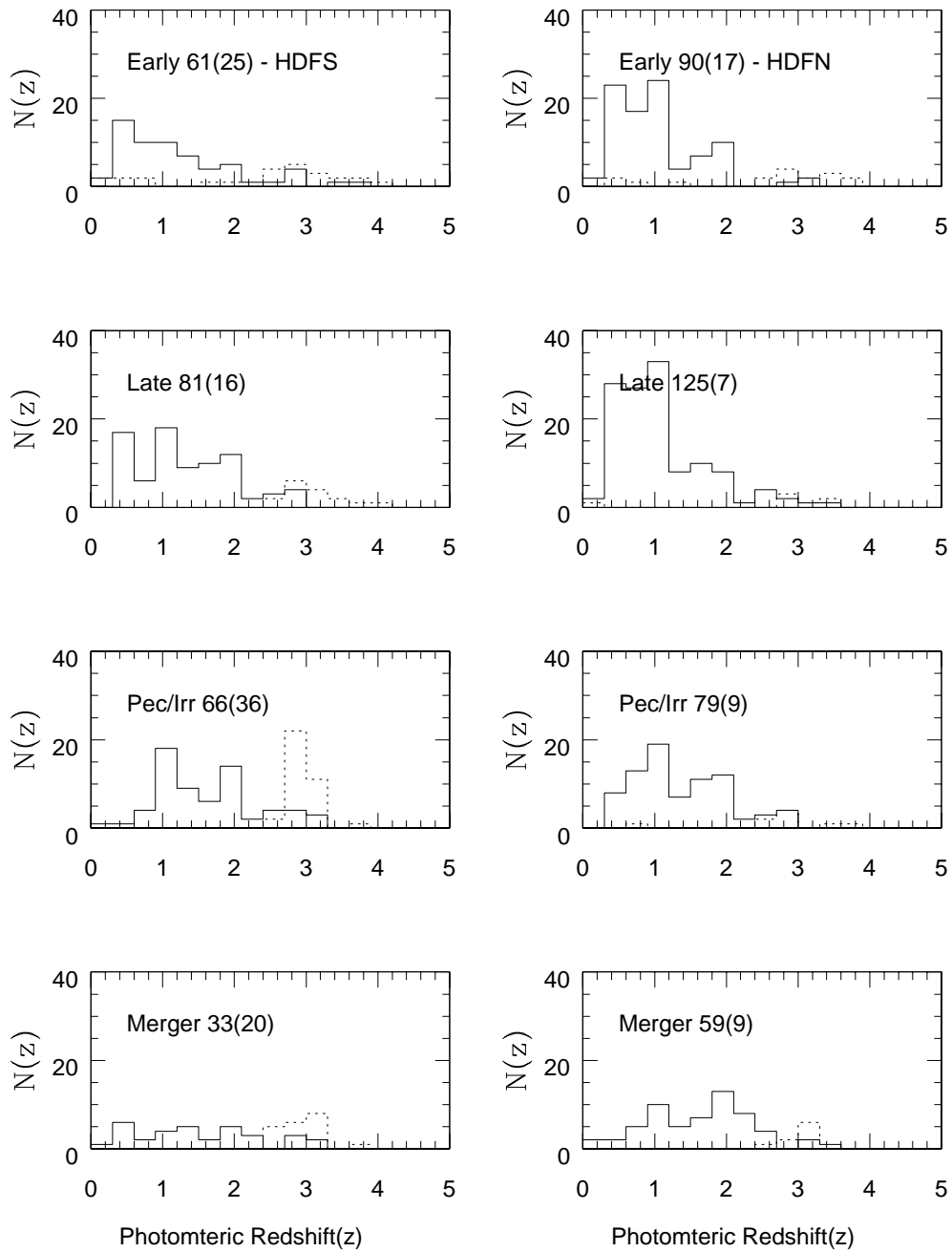


Fig. 6: Morphological redshift distribution of the galaxies with $I < 26$ mag in the HDFS (left) and the HDFN (right). The dotted lines represent the U -band limited galaxies and the numbers inside the parentheses represent the numbers of these galaxies.

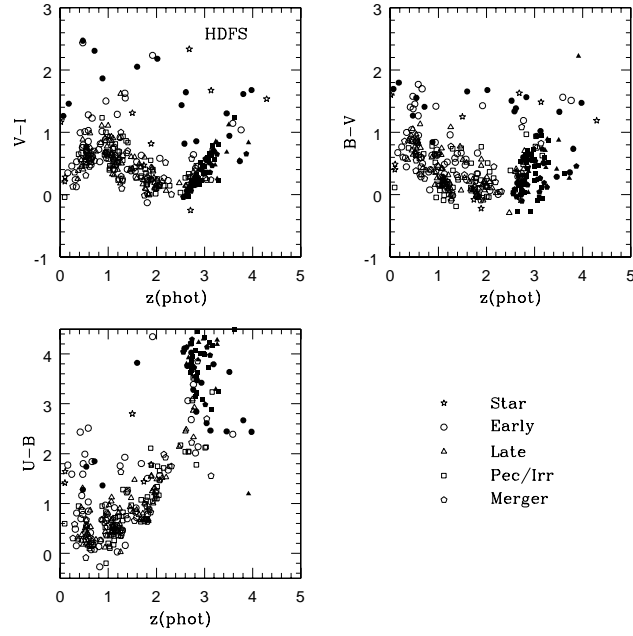


Fig. 7: Morphological color-redshift diagrams of the galaxies with $I < 26$ mag in the HDFs. Filled symbols represent the U -band limited galaxies.

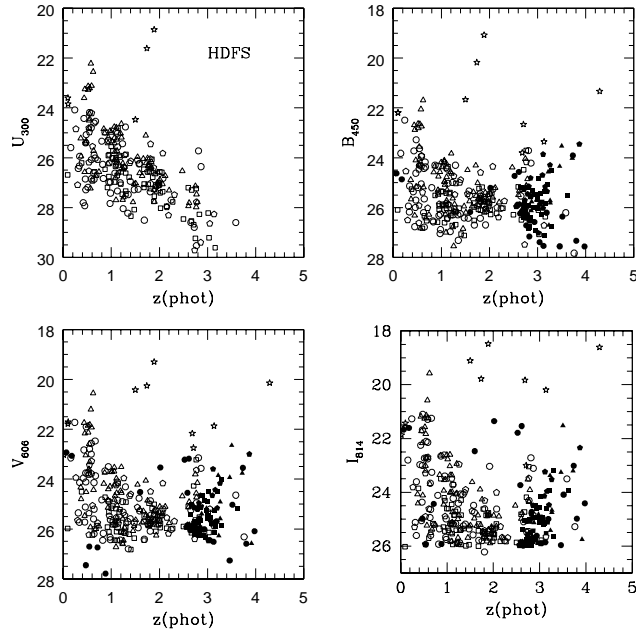


Fig. 8: Morphological magnitude-redshift diagrams of the galaxies with $I < 26$ mag in the HDFs. Filled symbols represent the U -band limited galaxies. Open symbols are the same as in Figure 7.